Imaging correlography with sparse arrays of detectors

J. R. Fienup, FELLOW SPIE
Environmental Research Institute of Michigan
Advanced Concepts Division
Optical Science Laboratory
P. O. Box 8618
Ann Arbor, Michigan 48107-8618

Paul S. Idell, MEMBER SPIE
Air Force Weapons Laboratory
Phased Array Branch (AFWL/ARBB)
Kirtland Air Force Base,
New Mexico 87117-6008

Abstract. Imaging correlography is a technique for constructing high resolution images of laser-illuminated objects from measurements of backscattered (nonimaged) laser speckle intensity patterns. In this paper, we investigate the possibility of implementing an imaging correlography system with sparse arrays of intensity detectors. The theory underlying the image formation process for imaging correlography is reviewed, emphasizing the spatial filtering effects that sparse collecting apertures have on the reconstructed imagery. We then demonstrate image recovery with sparse arrays of intensity detectors through the use of computer experiments in which laser speckle measurements are digitally simulated. It is shown that the quality of imagery reconstructed using this technique is visibly enhanced when appropriate filtering techniques are applied. The signal-to-noise ratio of the process and its dependency on array redundancy and number of speckle pattern measurements is also discussed.

Subject terms: multiple-aperture optical systems; speckle phenomena; intensity interferometry; phase retrieval; image reconstruction; synthetic apertures; atmospheric optics; Fourier transforms; statistical optics.

Optical Engineering 27(9), 778-784 (September 1988).

CONTENTS

1. INTRODUCTION

One can obtain large optical apertures, necessary to achieve high resolution imagery, by synthesizing a phased array of smaller optical elements or subapertures.[1-4] If the array is sparse (only partially filled), the modulation transfer function (MTF) of the system will generally be depressed at the middle and higher spatial frequencies, as compared with a filled aperture having the same diameter, resulting in loss of image contrast and resolution. Imagery obtained in this fashion can, in principle, be digitally postprocessed to remove the image distorting effects of the sparse collecting aperture through "MTF boosting." To ensure that the noise is not boosted more than the image signal, one should design the phased-array imaging system so that the synthesized MTF is greater than the detector noise threshold for all spatial frequencies of interest.

We have suggested a new optical imaging technique that constructs images of coherently illuminated, diffuse objects from measurements of (nonimaged) backscattered laser energy.[5,6] Recently, it was demonstrated in the optical laboratory.[7] This technique, which we call imaging correlography, uses measurements of the intensity of the coherent speckle pattern formed when an object is illuminated with a laser to calculate an estimate of the energy (or power) spectrum of the underlying incoherent object without requiring a phased array. An iterative Fourier transform algorithm is used to retrieve the phase associated with the square root of this energy spectrum to arrive at the complex Fourier transform of the incoherent object from which an unspeckled image is formed. Since this method relies on correlations of Fourier (pupil) plane speckle intensity, one can show that the estimate of the object's energy spectrum is filtered by a transfer function given by the autocorrelation of the pupil (the collecting area over which the speckle intensity is measured). As a consequence of this fact, we conclude that imaging correlography can be implemented with sparse collecting arrays of intensity detectors and that—with analogy to MTF boosting with phased-array, incoherent imaging systems—the speckle intensity data used in imaging correlography can be digitally processed to compensate for vacancies in the collecting aperture.

Invited Paper MA-115 received June 1, 1988; revised manuscript received June 11, 1988; accepted for publication July 15, 1988; received by Managing Editor July 21, 1988. This paper is a revision of Paper 828-21, presented at the SPIE conference Digital Image Recovery and Synthesis, Aug. 17-18, 1988, San Diego, Calif. The paper presented there appears (unrefereed) in SPIE Proceedings Vol. 828.

In this paper, we demonstrate that imaging correlography may be implemented with sparse arrays of Fourier plane detectors, as suggested above, and that MTF boosting of the estimated energy spectrum of the illuminated object has the desired effect of reducing image artifacts due to collecting array sparsity. We illustrate the effects of MTF boosting using computer simulations of the imaging correlography process. We also discuss the requirements for the product of array redundancy and number of speckle measurements needed to achieve an adequate signal-to-noise ratio.

2. IMAGING CORRELOGRAPHY

We begin with a review of the theory underlying the imaging correlography technique previously reported in Refs. 5 and 6. The material provided here is presented in a slightly different (although equivalent) mathematical form from that reported earlier in order to emphasize the role that a sparse collecting aperture plays in filtering the estimate of the object's energy spectrum.

Image synthesis using imaging correlography is based on the fact that the autocorrelation function of the illuminated object's brightness distribution can be obtained from the average energy spectrum of a laser speckle pattern.[8] (The brightness distribution is essentially the object's irradiance distribution had the object been illuminated with an incoherent light source.) Since the Fourier transform of the autocorrelation of the object's brightness function is equal to the squared modulus of the Fourier transform of the brightness function,[9] an image of the object can be obtained if the phase associated with this Fourier transform can be determined. To obtain this phase, we use the iterative transform algorithm, which employs the Fourier modulus estimated from the speckle data, together with the constraint that the object's brightness function be real valued and nonnegative.[10–12] Once the phase associated with the Fourier modulus is determined, the image is recovered by inverse transformation of the synthesized Fourier plane data. Because the image is recovered from an estimate of the energy spectrum of the object's brightness distribution, we find that the recovered image is unspeckled, even though the data for imaging correlography was obtained from measurements of coherent laser speckle intensity.

Rather than relating, as we did above, the average energy spectrum of the speckle pattern to the autocorrelation function of the object's brightness function, one can equate the autocovariance of the far-field laser speckle pattern with the energy spectrum of the object's brightness function. This second interpretation suggests the following procedure for image recovery: (1) estimate the autocovariance of the observed speckle intensity, (2) take the square root of the estimated autocovariance, (3) recover the phase associated with this square root, and (4) inverse Fourier transform the assembled Fourier data. Image recovery using this prescription uncovers a close relationship between imaging correlography and image recovery from intensity interferometry,[13] in which the object's Fourier phase information, too, is lost in the measurement process. (The fact that Fourier domain image information of incoherent objects can be obtained from far-field correlations is, of course, a consequence of the Van Cittert-Zernike theorem.[14])

We can demonstrate the relationship between the autocovariance of the laser speckle pattern and the object energy spectrum by considering the measurement process involved in

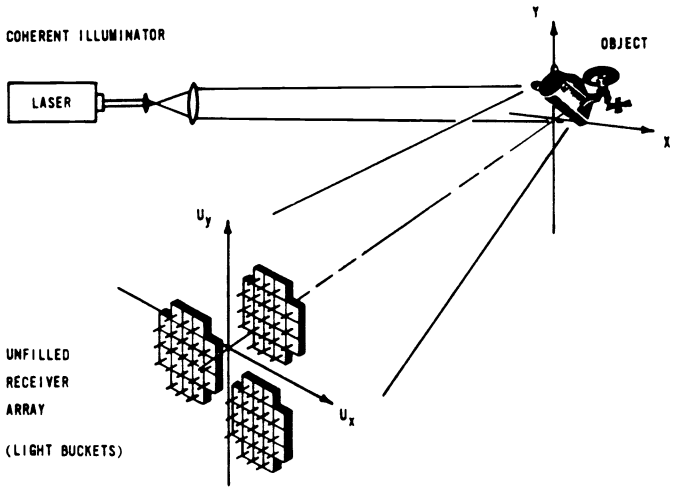

Fig. 1. Sensing geometry for a sparse-array implementation of imaging correlography. Light from the laser is expanded to flood illuminate the target object. The backscattered laser speckle intensity is measured with light bucket detectors arranged in an unfilled, two-dimensional array configuration.

imaging correlography. Let us suppose that a diffuse object is flood illuminated with a laser so that the object lies entirely within the coherence volume of the laser beam. A two-dimensional array of photodetectors measures the backscattered light intensity in a (far-field) plane some distance z from the object (see Fig. 1 for a possible measurement scenario). We assume that the object is optically rough so that its microscale surface height variations are random and of a size comparable with or greater than the wavelength of light. Additionally, we assume that the transverse scale size of the surface height fluctuations is small compared with the resolution patch size associated with the collecting array (i.e., the spatial correlation of surface roughness is small compared to $\lambda z/D$, where λ is the wavelength of light, z is the range, and D is the largest array dimension). This being the case, the reflected laser light is randomly (and coherently) dephased, and the photodetectors in the observation plane record the intensity pattern of a fully developed laser speckle pattern.[15]

Each realization of the observed speckle pattern $I_n(u)$ may be expressed as the squared modulus of the Fourier transform of the complex object field:

$$I_n(u) = |F_n(u)|^2 = |\mathcal{F}[f_n(x)]|^2 , \tag{1}$$

where $\mathcal{F}$ denotes a Fourier transform, $f_n(x) = |f_0(x)|\exp[i\phi_n(x)]$ is the field reflected by the object, $|f_0(x)|$ is the object's field amplitude reflectivity, and $\phi_n(x)$ is the (random) phase of the *nth* realization of the reflected object field associated with the object's surface height profile. (Independent realizations of the observed speckle intensity can occur if the object and measurement planes are laterally displaced with respect to each other or if the object rotates slightly.) In the above expression, x represents a two-dimensional spatial (or angular) coordinate vector in object space, and u represents a two-dimensional coordinate in the measurement plane. An estimate of the autocovariance of the measured speckle pattern may be computed as follows from N realizations of the laser speckle intensity:

$$\hat{C}_I(\Delta u;N) \equiv \frac{1}{N}\sum_{n=1}^{N}\int\int_{-\infty}^{\infty} P(u+\Delta u)P(u)[I_n(u+\Delta u)I_n(u) - \bar{I}^2]d^2u$$

$$= \int\int_{-\infty}^{\infty} P(u+\Delta u)P(u)\left\{\frac{1}{N}\sum_{n=1}^{N}[I_n(u+\Delta u)\, I_n(u) - \bar{I}^2]\right\}d^2u\,, \quad (2)$$

where $\bar{I}$ is the average intensity of the observed speckle pattern, Δu is a vector separation in the measurement plane, and $P(u)$ is the pupil (aperture) function associated with the collecting array, defined as

$$P(u) = \begin{cases} 1\,, & \text{for } u \in \text{aperture array}\,, \\ 0\,, & \text{otherwise}\,. \end{cases} \quad (3)$$

In the limit as N (the number of independent observed speckle patterns) approches infinity, one can use the moment factoring theorem for circular-complex Gaussian (ccg) fields[16] to show that

$$\lim_{n\to\infty}\frac{1}{N}\sum_{n=1}^{N}[I_n(u+\Delta u)I_n(u) - \bar{I}^2] = |\Gamma(\Delta u)|^2\,, \quad (4)$$

where $\Gamma(\Delta u) = \mathcal{F}[|f_0(x)|^2]$ is the Fourier transform of the object's brightness distribution [i.e., $\Gamma(\Delta u)$ is the mutual intensity of the (complex) speckle field in the measurement aperture, evaluated at field points separated by a vector Δu]. Our ability to invoke the ccg moment theorem above follows from the fact that the observed speckle field is ccg since the speckle pattern is fully developed. In the limit $N \to \infty$, we therefore find from Eqs. (2) and (4) that the estimated autocovariance of the speckle intensity observed over the measurement aperture $P(u)$ is given by

$$C_I(\Delta u) \equiv \lim_{N\to\infty}\hat{C}_I(\Delta u;N)$$

$$= \text{OTF}(\Delta u)|\Gamma(\Delta u)|^2\,, \quad (5)$$

where $\text{OTF}(\Delta u)$ is the autocorrelation of $P(u)$. This result demonstrates that $\hat{C}_I(\Delta u;N)$ provides an estimate for $|\Gamma(\Delta u)|^2$, the energy spectrum of the object's brightness function—the square root of which is an estimate of the Fourier modulus of the object's brightness function. This square root is used in the iterative transform algorithm to retrieve the associated Fourier phase data and thereby reconstruct an image.

We see from Eq. (5) that the estimated autocovariance of the observed speckle pattern provides a weighted, or filtered, estimate of the object's energy spectrum. This weighting is completely determined by the spatial arrangement of the detectors making up the collecting aperture. Because this weighting function $\text{OTF}(\Delta u)$ is equal to the autocorrelation of the measurement pupil, we refer to $\text{OTF}(\Delta u)$ as the optical transfer function (OTF) for the imaging correlography system—with obvious analogy to the OTF arising in the analysis of incoherent imaging systems. The MTF is just the modulus of the OTF, and, since the OTF is nonnegative, $\text{MTF}(\Delta u) = \text{OTF}(\Delta u)$. The fact that this OTF is in the form of an autocorrelation allows us to consider the use of sparse arrays of intensity detectors in imaging correlography.

3. APPLICATON TO SPARSE COLLECTING APERTURES

The fact that the OTF for imaging correlography is given by the autocorrelation of the pupil function $P(u)$ suggests a procedure with which to remove sidelobe artifacts introduced by a multiple-aperture (sparse array) measurement scheme. If the detector elements are positioned so that the autocorrelation of the detector array does not drop to zero within the bandpass of the OTF, the object energy spectrum estimated by the imaging correlography process contains essentially the same spatial frequencies as a filled aperture having the same diameter as the sparse array. And provided that the noise in the estimated autocovariance is not too great, the energy spectrum estimate can be boosted to match the OTF of a completely filled aperture; an image with nearly the resolution of the full aperture is then, in theory, synthesized.

In practical applicatons of imaging correlography, noise in the Fourier modulus estimate will arise from many sources, including detector noise, background flux noise, photon shot noise, and noise introduced when a finite number of speckle measurements is used to estimate the speckle autocovariance. Were all the noise sources additive and uncorrelated with the signal component, one would logically implement the MTF boosting procedure by applying a Wiener-Helstrom filter[17] to the Fourier modulus estimate so that the mean-square error between the estimated image and the true (full-resolution) image is minimized. Even if the signal and noise sources do not exactly satisfy these conditions, a Wiener-Helstrom filter is still very advantageous to use.[17]

For conventional incoherent imaging systems the Wiener-Helstrom filter is of the form

$$W(\Delta u) = \frac{\text{OTF}(\Delta u)|\Gamma(\Delta u)|^2}{|\text{OTF}(\Delta u)|^2|\Gamma(\Delta u)|^2 + E_n(\Delta u)}\,, \quad (6)$$

where $|\Gamma(\Delta u)|^2$ is the energy spectrum of the object's brightness function, $\text{OTF}(\Delta u)$ is the OTF of the collecting aperture, and $E_n(\Delta u)$ is the energy spectrum of the image-domain noise. This filter is based on a model of the imaging process, which is given in the Fourier domain as $\text{OTF}(\Delta u)\Gamma(\Delta u)$ + noise. However, a better model for imaging correlography is

$$\hat{C}_I(\Delta u;N) = \text{OTF}(\Delta u)|\Gamma(\Delta u)|^2 + N_c(\Delta u)\,, \quad (7)$$

where $N_c(\Delta u)$ is additive noise, for which the appropriate filtering operation to estimate the object's energy spectrum is

$$|\hat{\Gamma}(\Delta u)|^2 = W_c(\Delta u)\hat{C}_I(\Delta u;N)\,, \quad (8)$$

where the filter is given by

$$W_c(\Delta u) = \frac{\text{OTF}(\Delta u)|\Gamma(\Delta u)|^4}{|\text{OTF}(\Delta u)|^2|\Gamma(\Delta u)|^4 + E_c(\Delta u)}\,, \quad (9)$$

with $E_c(\Delta u)$ being the variance of $N_c(\Delta u)$.

Whether taking the square root of the speckle autocovariance and then filtering with Eq. (6) or filtering the speckle autocovariance with Eq. (9) and then taking the square root, the MTF is boosted where the signal-to-noise ratio is high and is depressed where the signal-to-noise ratio is low, thereby resulting in a better Fourier modulus estimate. Indeed, results of the computer simulations presented in the next section

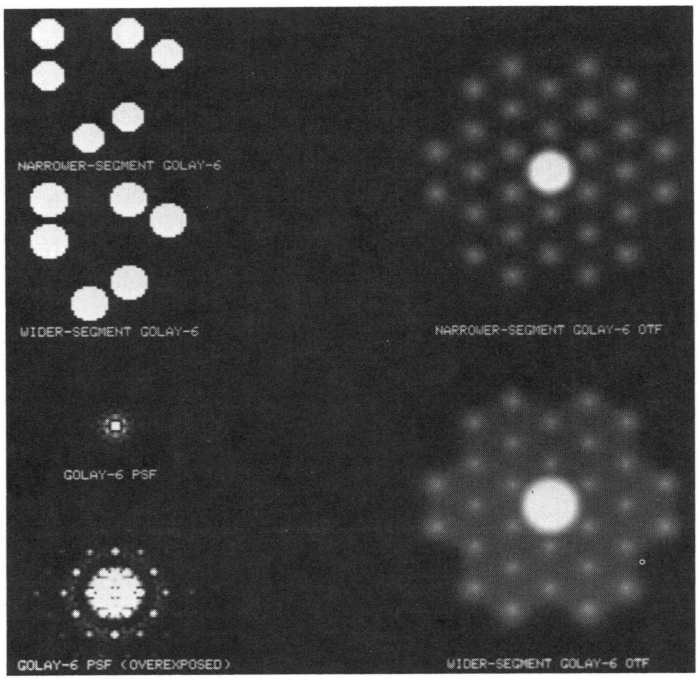

Fig. 2. Golay configurations containing six subapertures. Upper left: aperture functions P(u) for the Golay-6. Right: OTFs corresponding to the Golay-6 aperture functions shown in the upper left. Lower left: point-spread function associated with the wider-segment Golay-6 aperture.

demonstrate that such filtering techniques improve the overall quality of imagery recovered in imaging correlography.

4. COMPUTER SIMULATIONS

We conducted a series of computer experiments to demonstrate that phase retrieval can be used to recover imagery from far-field speckle intensity data collected over a sparse array. The procedure followed here is essentially the same as that reported in Refs. 5 and 6, with the exception that here the speckle realizations used to compute an estimate of the incoherent object's energy spectrum are masked with a pupil function P(u) emulating a sparse collecting array.

The original object data for these experiments were contained in a digitized photograph of a satellite model illuminated with incoherent light [see Figs. 4(G) and 5(G)]. The object's brightness function was represented by an array of approximately 40×60 pixels imbedded in a 128×128 discrete array. Each realization of a (coherent) speckled image of the object was obtained from the digitized photograph by (1) replacing each pixel with a circular-complex Gaussian random variable having a variance for the real and imaginary parts each equal to half the original pixel brightness value and (2) low pass filtering the result. The filter used to smooth the complex object data corresponds to the pupil function P(u) that defines the detector array area in the measurement aperture. For the sparse aperture simulations, we used a Golay-type array[18] comprising six subapertures. Figure 2 shows the Golay aperture configurations used for this study together with the corresponding OTFs and point-spread functions. The narrower- and wider-segment Golay arrays were both configured to have a 16 pixel separation between adjacent subapertures; the diameters of the individual subapertures in the narrower- and wider-segment arrays were 11 and 13 pixels, respectively.

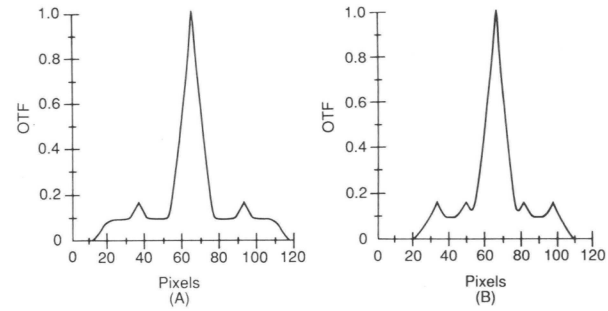

Fig. 3. Cross sections of the wider-segment Golay-6 aperture. (A) Horizontal cut through origin of OTF pictured in Fig. 1; (B) vertical cut through origin.

In both cases the OTF, which is the autocorrelation of the pupil function, consists of a large central peak surrounded by 30 satellite peaks. Although the widths of the subapertures for both cases were chosen to be large enough that the OTF does not drop to zero within the bandpass, the narrower-segment array OTF does drop to low values in the regions between the satellite OTF peaks. In the presence of noise, these dips in the OTF could result in information loss at these spatial frequencies. For the wider-segment case, the OTF stays above half the value of the satellite peaks in the areas between the satellite peaks, as can be seen in Fig. 3. For this reason the wider-segment Golay array was chosen for the simulation. To perform the filtering operation on the complex object data, the sampled Golay arrays were embedded in a 128×128 array. Multiple realizations of the coherent object data were then obtained by using different random number seeds in the computation of the complex Gaussian random variables.

An estimate of the object energy spectrum was formed by processing multiple arrays of pupil-plane speckle intensity data computed from realizations of the filtered coherent object. Several different estimators of the object energy spectrum can be used, such as the one given by Eq. (2). For these experiments, first the average energy spectrum of the speckle intensity was computed by inverse Fourier transforming the squared modulus (i.e., the speckle intensity) of the Golay-apertured Fourier transform for each simulated coherent image, and then these speckled energy spectra were averaged together. After a large number N of independent coherent speckle data sets were processed in this fashion, a dc term (in fact a function, corresponding to a scaled version of the squared modulus of an average of the Fourier transforms of the windowed speckle intensity arrays observed over the measurement aperture) was subtracted, and the result was Fourier transformed, providing an estimate of the autocovariance of the observed speckle pattern, which by Eq. (5) is an OTF-weighted estimate of the incoherent object's energy spectrum.

Results of image reconstruction experiments applying phase retrieval to the estimate of the object's energy spectrum are shown in Fig. 4. Figure 4(A) shows the averaged energy spectrum (with the dc term removed) of the pupil-plane speckle intensity for the wider-segment Golay-6 array shown in Fig. 2, for which N = 10,240 independent realizations of speckle intensity were averaged. Figure 4(B) is an estimate of

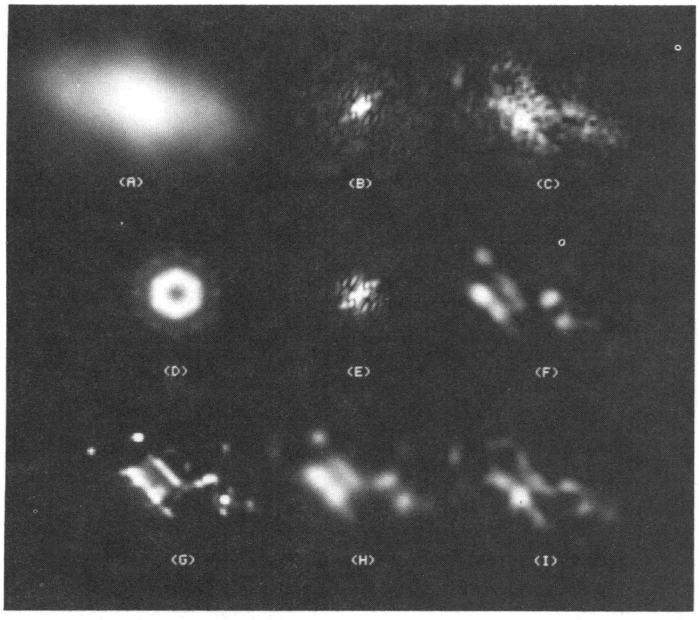

Fig. 4. Image recovery using the Golay-6 aperture, N = 10,240. (A) Average energy spectrum of the measured speckle patterns (with dc term removed); (B) estimate of the Fourier modulus of the object brightness distribution; (C) image reconstructed from 4(B) using the iterative transform (phase retrieval) algorithm; (D) Wiener-like filter for the Golay-6 aperture; (E) filtered Fourier modulus estimate; (F) image reconstructed from 4(E); (G) original incoherent object; (H) filtered incoherent object; (I) result of filtering 4(C).

the Fourier modulus of the object's brightness distribution computed by taking the square root of the Fourier transform of Fig. 4(A). Negative numbers, resulting from noise associated with the finite-average approximation to an ensemble average, were set to zero prior to taking the square root. Figure 4(C) is the image produced by applying the iterative transform phase retrieval algorithm[10–12] to the Fourier modulus data contained in Fig. 4(B). The procedure for accomplishing phase retrieval involved applying several cycles of the hybrid input-output algorithm (using $\beta = 0.7$) and the error reduction algorithm until the algorithm appeared to stagnate. The object-domain constraints used were nonnegativity (since an unspeckled, or incoherent, image is being reconstructed) and a loose support constraint, a rectangle half the size of the smallest rectangle enclosing the average energy spectrum of the observed speckle pattern. The object is guaranteed to fit within this support constraint.[19]

Note that the recovered image shown in Fig. 4(C) is very noisy compared with the original incoherent object, shown in Fig. 4(G), although a general semblance of the object has been recovered. Noise in this reconstructed image is due to the fact that a finite (albeit large) number of speckle realizations were used to estimate the Fourier modulus. To reduce these noise effects, we multiplied the Fourier modulus estimate shown in Fig. 4(B) by the Wiener-like filter of Eq. (6). For these simulations, the energy spectrum of the object was taken to be an angular (spin) average over the squared Fourier modulus of the true object. The noise spectrum was approximated by a constant whose value was obtained by averaging the squared Fourier modulus estimate over those higher spatial frequencies where the signal-to-noise ratio was less than one. Figure 4(D) shows the resulting Wiener filter used for this example. Figure 4(E) shows the product of the filter of Fig. 4(D) with the original Fourier modulus estimate of Fig. 4(B).

Figure 4(F) shows the image reconstructed from the filtered Fourier modulus estimate in Fig. 4(E) using the phase retrieval algorithm. Note that the filter has significantly improved the quality of the reconstructed image in Fig. 4(F) over that in Fig. 4(C) reconstructed without filtering. For the purposes of comparison, the original object in Fig. 4(G) was passed through the filter in Fig. 4(D), with the result shown in Fig. 4(H). The image reconstructed from speckle correlation measurements, shown in Fig. 4(F), compares favorably with the filtered object in Fig. 4(H), indicating good performance on the part of the iterative transform algorithm. Figure 4(I) shows the result of applying the Wiener filter to the reconstructed image shown in Fig. 4(C). It appears, at least for this example, that filtering followed by image reconstruction is somewhat superior to image reconstruction followed by filtering. We might expect to get even better results by using an improved Wiener filter, for example, by using a better estimate of the object power spectrum or by using Eqs. (8) and (9).

One way to evaluate the MTF-boosting properties of the filter of Eq. (6) is by inspection of the filter, which is shown in Fig. 4(D). Notice that it has a local minimum in the center (at zero spatial frequency) and a ring of local maxima at a higher spatial frequency. This compensates, in part, for the rapid drop-off of the OTF that can be seen in Fig. 3. The ratio of the peak value of the filter to the zero-frequency value is 3.38, a sizable boosting of the OTF at that spatial frequency. This falls short of a complete compensation due to the noise energy spectrum term in Eq. (6). For the same reason, the filter drops off for the highest spatial frequencies, where the noise dominates the signal.

Another way to evaluate the MTF-boosting properties of the filter of Eq. (6) is to compare the imaging results shown in Fig. 4 with those obtained with a filled collecting aperture. Figure 5 shows the results of image recovery from simulations of imaging correlography obtained with a filled aperture, in which the simulated speckle intensity data were filtered by a square aperture comprising 64×64 "detector" pixels fully encompassing the sparse Golay aperture used above. (The width of the Golay array is only 55 pixels.) The results shown in Fig. 5 are those reported in Refs. 5 and 6. Except for the form of filtering used to mask the speckle measurement data, the digital processing steps used to produce each frame of Fig. 5 is identical to that of the corresponding frame of Fig. 4. The top row of frames of Fig. 5 correspond to image retrieval with a full aperture but without Wiener filtering. Note that the resulting image in Fig. 5(C) is noisy but is significantly better than its sparse array counterpart in Fig. 4(C). The filter shown in Fig. 5(D) is that prescribed by Eq. (6), with the OTF given by the autocorrelation of the filled square aperture. Figure 5(F) shows the image recovered from the Wiener-filtered Fourier modulus in Fig. 5(E) for the filled aperture. Comparing Figs. 4(F) and 5(F) indicates that most of the key features of the object recovered in the filled-aperture case were also recovered with the sparse Golay-6 aperture case. However, some of the finer details of the object recovered in the full aperture case were smoothed over in the Golay aperture reconstruction. This loss of resolution for the sparse-aperture case is the result of a smaller OTF(Δu) value (i.e., a lower

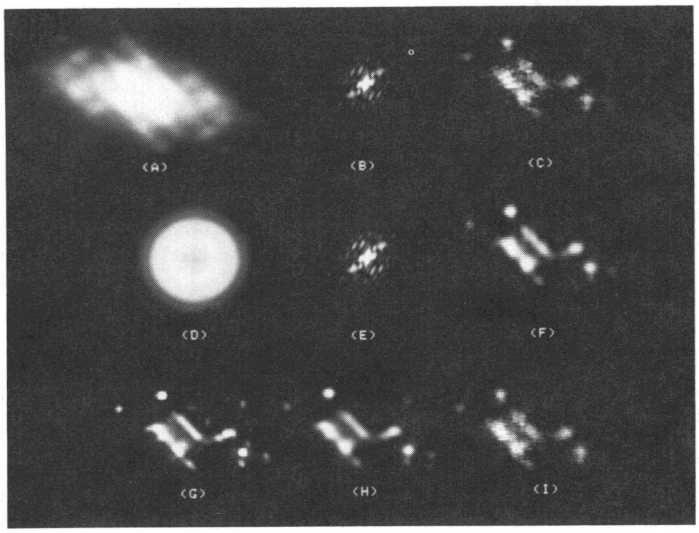

Fig. 5. Image recovery using a filled aperture, N = 10,000. (A) Average energy spectrum of the measured speckle pattern (with dc term removed); (B) estimate of the Fourier modulus of the object brightness distribution; (C) image reconstructed from 5(B) using the iterative transform (phase retrieval) algorithm; (D) Wiener-like filter for the filled aperture; (E) filtered Fourier modulus estimate; (F) image reconstructed from 5(E); (G) original incoherent object; (H) filtered incoherent object; (I) result of filtering 5(C).

redundancy), and hence a lower signal-to-noise ratio, for larger spatial frequencies.

The results of this section demonstrate the possibility of recovering images from nonimaged (far-field) laser speckle patterns observed with sparse arrays of intensity detectors. The images obtained using a combination of a Wiener-filtered speckle autocovariance together with the iterative transform phase retrieval algorithm show marked improvement over those obtained without filtering. The fact that the image in Fig. 4(F), constructed with sparse arrays of detectors, approaches the quality of the full-aperture image in Fig. 5(F) suggests that the MTF boosting filter is successful in removing image artifacts due to the sparse collecting aperture.

5. SIGNAL-TO-NOISE RATIO AND RESOLUTION

Up to this point, we have not addressed the role that the number N of independently observed speckle patterns plays in the quality of images recovered in imaging correlography. It is clear that the error in the speckle autocovariance, and so the Fourier modulus estimate, will improve as the number of speckle measurements increases, whether these speckle measurements arise from additional speckle pattern realizations (snapshots) or from an increased redundancy in the OTF of the collecting aperture. This flexibility in choosing between the number of snapshots N and the collecting array redundancy can be better appreciated by considering the signal-to-noise ratio (SNR) of the autocovariance estimate achieved in imaging correlography. Assuming that time-sequential measurements of the speckle patterns are statistically independent, one can show that the SNR of the estimate of the object's energy spectrum at spatial frequency Δu provided by the estimator of Eq. (2) is given by[20]

$$\mathrm{SNR}_C(\Delta u;N) = \frac{(NK)^{1/2}|\mu(\Delta u)|^2}{[3 + 14|\mu(\Delta u)|^2 + 3|\mu(\Delta u)|^4]^{1/2}}, \tag{10}$$

where N is the number of independent speckle patterns (snapshots) observed, $\mu(\Delta u) = \Gamma(\Delta u)/\Gamma(0)$ is the complex coherence factor for the measured speckle field, and

$$K = K(\Delta u) = N_p \mathrm{OTF}(\Delta u) \tag{11}$$

is the number of redundant pairs of speckle intensity in the collecting aperture measured at pixel separation Δu. In the above, N_p is the number of independent samples of intensity (or number of speckles) contained in the measurement aperture P(u). For the case in which the noise in the Fourier modulus estimate is dominated by statistical fluctuations in the autocovariance estimate itself (not by photon shot noise, etc.), Eq. (10) specifies the tradeoff between array redundancy K and number of speckle snapshots N needed to keep the SNR of the estimate at an acceptably high level. Keeping the SNR of the speckle autocovariance, and so the SNR of the estimate of the object's Fourier modulus, at a high level will preserve an acceptable quality in the image recovered using the iterative transform phase retrieval algorithm.

The above noise analysis included only the effects of approximating the ensemble average by averaging over a finite number of realizations. The variance of the noise that includes both finite averaging noise and photon noise is given by $(NK)^{-1}$ times[21]

$$(3 + 14|\mu|^2 + 3|\mu|^4) + \left[\frac{4(1 + 2|\mu|^2)}{M\langle n\rangle} + \frac{1 + |\mu|^2}{M\langle n\rangle^2}\right],$$

where the first set of terms is due to finite averaging and the second is due to photon noise, M is the number of detectors (pixels) per speckle, and $\langle n\rangle$ is the mean number of photons per detector. Thus, for $|\mu|^2 \ll 1$, the finite averaging noise variance is proportional to 3, while the photon noise variance is proportional to $4/(M\langle n\rangle) + 1/(M\langle n\rangle^2)$. For M = 4, the two noise variances are equal for $\langle n\rangle = \frac{1}{2}$ photon per detector or $M\langle n\rangle = 2$ photons per speckle. Consequently, independent of the array redundancy and the number of realizations, photon noise will be negligible as long as the number $M\langle n\rangle$ of photons per speckle is much greater than two.

6. SUMMARY

We have demonstrated via computer simulations that it is possible in principle to recover an incoherent image of a laser-illuminated object from multiple realizations of detected speckle intensities collected over sparse arrays. This would permit the reconstruction of fine-resolution images despite phase errors due to atmospheric turbulence. The expressions for signal-to-noise ratio as a function of spatial frequency, array redundancy, and number of speckle realizations show that large amounts of array redundancy and/or large numbers of speckle realizations are required to reconstruct an image of large space-bandwidth product.

7. ACKNOWLEDGMENTS

The authors wish to acknowledge the contributions of Ron S. Goodman of the Environmental Research Institute of Michigan, who conducted the computer simulations shown herein. This work was supported by the Air Force Weapons Laboratory, partially through Air Force Wright Aeronautical Laboratory contract F33615-83-C-1046.

8. REFERENCES

1. J. W. Goodman, "Synthetic aperture optics," in *Progress in Optics*, Vol. VIII, E. Wolf, ed., North-Holland, New York (1970).
2. A. Meinel, M. Meinel, and N. Woolf, "Multiple aperture telescope diffraction images," in *Applied Optics and Optical Engineering*, Vol. IX, R. Shannon and J. Wyant, eds., Academic Press, New York (1983).
3. J. E. Harvey, P. R. Silverglate, and A. B. Wissinger, "Optical performance of synthetic aperture telescope configurations," in *Southwest Conference on Optics*, R. S. McDowell, ed., Proc. SPIE 540, 110–118 (1985).
4. G. O. Reynolds, "A review of partially-filled, synthetic-aperture imaging systems," in *Infrared, Adaptive, and Synthetic Aperture Optical Systems*, R. B. Johnson, W. L. Wolfe, and J. S. Fender, eds., Proc. SPIE 643, 141–179 (1986).
5. P. S. Idell and J. R. Fienup, "Imaging correlography: a new approach to active imaging," in *Proc. Twelfth DARPA Strategic Systems Symposium* Riverside Research Institute, Oct. 28–30, 1986, pp. 141–151, Naval Postgraduate School, Monterey, Calif.
6. P. S. Idell, J. R. Fienup, and R. S. Goodman, "Image synthesis from nonimaged laser speckle patterns," Opt. Lett. 12, 858–860 (1987).
7. P. S. Idell, J. D. Gonglewski, D. G. Voelz, J. Knopp, and B. Speilbusch, "Image synthesis from nonimaged laser speckle patterns: experimental verification," J. Opt. Soc. Am. A 4(13), P127 (1987).
8. L. I. Goldfischer, "Autocorrelation function and power spectral density of laser-produced speckle patterns," J. Opt. Soc. Am. 55, 247–253 (1965).
9. R. N. Bracewell, *The Fourier Transform and Its Applications*, McGraw-Hill (San Francisco), 115 (1978).
10. J. R. Fienup, "Reconstruction of an object from the modulus of its Fourier transform," Opt. Lett. 3, 27–29 (1978).
11. J. R. Fienup, "Phase retrieval algorithms: a comparison," Appl Opt. 21, 2758–2769 (1982).
12. J. R. Fienup and C. C. Wackerman, "Phase retrieval stagnation problems and solutions," J. Opt. Soc. Am. A 3, 1897–1907 (1986).
13. R. Hanbury-Brown, *The Intensity Interferometer*, Taylor and Francis, London (1974).
14. J. W. Goodman, *Statistical Optics*, p. 207, Wiley, New York, (1985).
15. J. W. Goodman, "Statistical properties of laser speckle patterns," in *Laser Speckle and Related Phenomena*, 2nd Edition, J. C. Dainty, ed., pp. 9–75, Springer-Verlag, New York (1984).
16. Ref. 14, pp. 73 and 271.
17. C. W. Helstrom, "Image restoration by the method of least squares," J. Opt. Soc. Am. 57, 297–303 (1967).
18. M. Golay, "Point arrays having compact nonredundant autocorrelations," J. Opt. Soc. Am. 61, 272–273 (1971).
19. J. R. Fienup, T. R. Crimmins, and W. Holsztynski, "Reconstruction of the support of an object from the support of its autocorrelation," J. Opt. Soc. Am. 72, 610–624 (1982).
20. J. C. Marron, "Accuracy of Fourier magnitude estimation from speckle intensity measurements," J. Opt. Soc. Am. A 5, 864–870 (1988).
21. K. O'Donnell, "Time-varying speckle phenomena in astronomical imaging and in laser scattering," Ph.D. thesis, Univ. of Rochester (1983).

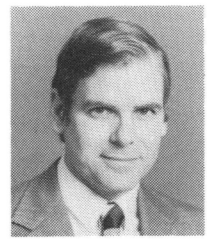

James R. Fienup received BA degrees in physics and mathematics (magna cum laude) from Holy Cross College, Worcester, Mass., in 1970 and the MS and Ph.D. degrees in applied physics from Stanford University in 1972 and 1975, respectively. He was a National Science Foundation Graduate Fellow from 1970 to 1972. His graduate work concerned a new type of computer-generated hologram. In 1975 he joined the Environmental Research Institute of Michigan, where he is currently a senior research physicist in the Optical Science Laboratory. His research activities include phase retrieval and image reconstruction algorithms, optical and digital image processing, and holographic optical elements. His publications include more than 50 technical papers. Dr. Fienup is a fellow of SPIE and OSA and is a member of the IEEE, Sigma Xi, and Sigma Pi Sigma. He is the recipient of the SPIE 1979 Rudolph Kingslake Medal and Prize and the International Commission for Optics 1983 International Prize in Optics. He has served as an associate editor of *Optics Letters* and as a feature editor of the *Journal of the Optical Society of America* (November 1983 and January 1987).

Paul S. Idell received a BSEE degree from Lehigh University in 1977 and an MSEE degree from the Air Force Institute of Technology, Wright-Patterson Air Force Base, Ohio, in 1978. From 1979 through 1983, he was assigned to the Rome Air Development Center, Griffiss Air Force Base, N.Y., where he managed various Air Force and DARPA sponsored research contracts related to optical and infrared sensor development. In 1986 he received a Ph.D. degree from Stanford University, where he concentrated on the areas of optical coherence theory and statistical optics. Currently stationed at the Air Force Weapons Laboratory at Kirtland Air Force Base, Dr. Idell conducts research into nonconventional, high resolution optical imaging techniques. He is active in SPIE, having chaired a recent SPIE conference on Digital Image Recovery and Synthesis (Proc. SPIE 828), and holds professional memberships in the OSA and IEEE.